# Journal of Materials Chemistry B

Accepted Manuscript






ROYAL SOCIETY OF CHEMISTRY

www.rsc.org/materialsB

Cite this: DOI: 10.1039/c0xx00000x

www.rsc.org/xxxxxx

ARTICLE TYPE

# Citric acid modification of PLLA nano-fibrous scaffolds to enhance cellular adhesion, proliferation and osteogenic differentiation

**Jundong Shao[a,b,c], Si Chen[a,b], and Chang Du*[a,b]**

***Received (in XXX, XXX) Xth XXXXXXXXX 20XX, Accepted Xth XXXXXXXXX 20XX***
**DOI: 10.1039/b000000x**

Citric acid (CA) was used during thermally induced phase separation (TIPS) process to improve the surface hydrophilicity and cell affinity of PLLA nano-fibrous scaffolds. The evolutions of architecture, structure and physicochemical properties of the scaffold after modification have been investigated. Cell viability, adhesion, proliferation and osteogenic differentiation were characterized to evaluate the cytocompatibility and biological properties of PLLA nano-fibrous scaffolds. Citric acid interacted with PLLA through hydrogen bond association and the introduction of strongly polar groups (−COOH) on PLLA surface improved its hydrophilicity with the contact angle decreasing to a suitable range for cell adhesion and spreading. The cell had extensive spreading on the CA modified PLLA scaffolds with many cellular protrusions interacting with nanofibers. Furthermore, such modification significantly increased cell proliferation rate, enhanced the alkaline phosphatase (ALP) activity and bone-related gene expression (ALP, OCN, COL I and Runx2) of mBMSCs along with the cell development. The results demonstrate a promising modification method to promote applications of PLLA-based scaffolds.

## Introduction

Nano-fibrous scaffolds of various biocompatible and biodegradable materials have been extensively studied in terms of promoting cell adhesion, proliferation and differentiation[1-6]. Their physicochemical properties such as high porosity and large surface area make them ideal for a variety of tissue engineering applications[7,8]. A thermally induced phase separation process has been successfully employed to produce nano-fibrous PLLA[9-11] scaffolds mimicking the fibrillar structure of collagen (50 to 500 nm in diameter) [12].

The basic features of tissue engineering scaffolds are to combine with cells. In addition to a variety of materials physical and chemical properties, the scaffolds should also have a good cellular affinity[13]. The specific interaction between cells and scaffolds results from molecular recognition between cell membrane receptor and ligand on the surface of scaffolds[14]. Surface properties include surface free energy, hydrophilicity/hydrophobicity, and surface chemical composition and charge etc. Different surface properties of materials can lead to different effects on cell adhesion, proliferation and differentiation[15-21].

As one of the most prominent biodegradable, biocompatible and environment-responsive polymer, Poly (L-lactic acid) (PLLA) has been attracting much attention in regards to their structure, properties and applications in the areas of drug delivery[8,11] and tissue engineering[9,10] from the academic viewpoint of fundamental researches as well as for practical applications. However, a strong hydrophobicity of PLLA put a major limitation to its cellular affinity[22], PLLA-derived scaffolds lack cell recognition signals and its hydrophobic nature hinders cell seeding[23,24]. In order to make the surface of PLLA scaffolds more conducive to cell activity, surface modifications such as grafting polymerization[25] and plasma technique[26] are expected to create cell-biomaterial interfaces that can elicit controlled cell adhesion, proliferation and/or maintain necessary differentiation. For example, wet chemical reactions, such as aminolysis and NaOH etching, were explored for PLLA surface modification[27]. The process generally used harsh conditions and sensitive to reaction temperature and duration. Plasma techniques such as oxygen plasma treatment and nitrogen plasma treatments provide a flexible and controllable method for PLLA surface modification, but it is generally used on films and with ageing and recovery effect[28], which may limit its application.

Citric acid (CA) is a weak organic acid with the formula $C_6H_8O_7$, which has three carboxyl (R-COOH) groups. The conjugate base of CA is important as an intermediate in the citric acid cycle, which occurs in the metabolism of all aerobic organisms. CA has therefore gained the approval of FDA for a variety of human clinical applications and has been widely used in biomaterials[29,30].

In this study, we focused on the surface modification of PLLA nano-fibrous scaffolds through the introduction of CA in order to get a better biocompatibility. PLLA-based nano-fibrous scaffolds

were prepared through thermally induced phase separation (TIPS) process. The interaction between PLLA and CA has been analyzed by investigating the surface topography and physical and chemical properties of the scaffolds. Biological evaluation was performed with regard to cell compatibility and osteogenic differentiation of stem cells.

## Experimental Section

### *Materials and reagents*

Poly (L-lactic acid) with a viscosity average molecular weight of 200,000 (inherent viscosity = 2.4 dl/g) was purchased from DaiGang Biomaterial Co. Ltd. (Shandong, China), and used as received. Citric acid (CA) was purchased from BaiShi Chemical Co. Ltd. (Tianjin, China). Tetrahydrofuran (THF) and all other chemicals were from DAMAO REAGENT (Tianjin, China). Deionized water was purified with a Milli-Q water purification system from Millipore Corporation (France). All reagents were of analytical reagent grade and were used directly without any further purification.

### *Preparation of scaffolds*

PLLA nano-fibrous scaffolds as a control group were prepared through TIPS process following the procedures of Ma et al[31]. In brief, a homogeneous polymer solution with a concentration of 4% (w/v%) was prepared by dissolving PLLA in THF. The solution was stirred at about 60 ℃ for 2 hours. Phase separation process was conducted at -24 ℃ for 2 hours. After complete gelation, deionized water was used for the solvent exchange at 4 ℃ and changed three times a day for 2 days. The resultant sample was then lyophilized for 48 hours to remove the water and residual solvent. Citric acid was introduced into the TIPS process and a variety of PLLA-based scaffolds were obtained following the similar procedures. The sample abbreviated with "PLLA/CA" was obtained by dissolving equal amounts of PLLA and CA in THF. The sample abbreviated with "PLLA/CA-CA" was obtained by further using a 0.5% (w/v%) CA solution instead of deionized water to exchange THF from PLLA/CA.

### *Scanning electron microscopy (SEM)*

Scanning Electron Microscope (NOVA NANOSEM430, FEI, the Netherlands) operating at 5-10 kV was used to examine the surface morphology of the samples. Before SEM examination, the samples were coated with gold for 120 s using a sputter coater (EM-SCD500, Leica, Germany).

Cells cultured on PLLA and PLLA/CA-CA scaffolds were rinsed with phosphate buffer saline (PBS) and then fixed with 2.5% glutaraldehyde in 0.1 M PBS for 4 hours at room temperature. The samples were then dehydrated in a series of ethanol (50%-100%) and sputter-coated with gold for SEM observation at 10 kV.

### *Contact angle measurement*

The hydrophilicity/hydrophobicity of all the samples were determined by static contact angle using the sessile drop method with a contact angle goniometer OCA20LHT-TEC700-HTFC1500 (Dataphysics, Germany). The contact angle measurement was performed on the as-synthesized samples. Furthermore, since the porous morphology may have certain effect on the contact angle measurement, all the samples were pressed into thin films and the pressed samples with quite small roughness were also tested.

### *Wide-Angle X-ray Diffraction (WAXD)*

The crystalline structures of all the samples were investigated by Wide angle X-ray diffraction (WAXD). WAXD patterns were taken on a Bruker D8 ADVANCE diffract-meter (Germany) with Cu-filtered Cu Kα radiation (λ = 0.1542 nm), operated at 40 kV and 40 mA under ambient conditions. The scan range was between 10 °and 50 °with the scan rate of 0.2 °/min.

### *Attenuated total reflectance FTIR (ATR-FTIR)*

The attenuated total reflectance Fourier-transform infrared (ATR-FTIR) analysis was performed on a Nicolet, CCR-1 FTIR spectrometer at room temperature. Standard crystal material, zinc selenide (ZnSe), was used as an internal reflection element with a fixed angle of incidence of 45 °. All the ATR-FTIR spectra were collected with 64 scans and measured at a 2 $cm^{-1}$ spectral resolution.

### *Cell culture and seeding*

The mouse bone marrow stromal cells (mBMSCs) were purchased from American Type Culture Collection (ATCC, Manassas, VA, USA). The cells were cultured in H-DMEM medium supplemented with 10% (v/v) fetal bovine serum (FBS). All cells were maintained in a 37 ℃ incubator with humidified atmosphere of 5% $CO_2$. The PLLA and PLLA/CA-CA scaffolds were sterilized by immersion in 70% (v/v) ethanol for 30 min, washed twice with PBS for 30 min each, and twice in fresh cell culture medium for 30 min each on an orbital shaker. Each PLLA-based scaffold (with dimensions of 8 mm in diameter and 2 mm in thickness) was seeded with $1\times10^4$ cells in 20 μl cell culture medium. After the initial 2 hours of cell seeding, the cell-scaffold constructs were placed in the wells of 24-well plates. Then 1 ml cell culture medium was added into each well. Medium was changed after the initial 24 h of seeding and culture, and then was changed every 2 days.

### *Cell proliferation and viability*

The cell viability on the scaffolds was evaluated using a Live/Dead Viability/Cytotoxicity Assay Kit, following the manufacturer's instruction. Cell proliferation was quantitatively examined using Cell Counting Kit-8 (CCK-8) assay. The absorbance was determined at 450 nm at a microplate spectrophotometer (Varioskan Flash 4.00.53, Finland) and used as an indicator of cell proliferation.

### *Alkaline phosphatase activity evaluation*

Alkaline phosphatase activity was evaluated as a marker for osteogenic differentiation of mBMSCs on PLLA and PLLA/CA-CA scaffolds. For osteogenesis, mBMSCs were seeded at a density of $2\times10^5$ cells/scaffold. Osteogenic induction was accomplished using H-DMEM supplemented with 10% FBS, 0.1 μM dexamethasone, 10 mM β-glycerophosphate disodium and 0.05 mM Vitamin C. The cell-scaffold constructs were cultured for up to 28 days with medium being replaced every 2-3

days. The constructs were evaluated at different time points respectively.

Cell-scaffold constructs were washed with PBS for 3 times and then immersed in embedding medium. After freezing at -24 ℃ for 30 min, the sample was cut into slices 5-20 μm in thickness by using a freezing microtome. The slice was immediately immersed in a fixative of 4% (w/v) paraformaldehyde at 4 ℃ for 20 min and then washed with 0.01 M PBS for 3 times (10 min/time). At last, the 5-bromo-4-chloro-3-indolyl phosphate/nitro blue tetrazolium (BCIP/NBT) solution was used for the alkaline phosphatase staining for about 30 min, and then observed under microscope.

Alkaline phosphatase (ALP) activity was further quantitatively determined using p-nitrophenyl phosphate (pNPP) assay. Briefly, cell-scaffold constructs were pre-washed with PBS, and then the adherent cells were removed from the scaffolds and lysed in 0.5 ml PBS containing 0.1 M glycine, 1 mM $MgCl_2$ and 0.05% Triton X-100 for 10 min at 4 ℃. The lysate was incubated with pNPP solution at 37 ℃ for 30 min, and then the absorbance was determined to indicate ALP concentration at 405 nm under a microplate spectrophotometer (Varioskan Flash 4.00.53, Finland). ALP activity was calculated according to manufacturer's instruction.

***Real-time quantitative reverse transcription-polymerase chain reaction (real-time RT-PCR)***

Total RNA was isolated from cells, which have been induced to osteogenic differentiation for 21 days and 28 days, using a HiPure Total RNA Kits (Magen) following TRIzol protocol. Then the RNA was subjected to reverse transcription with PrimeScript RT reagent Kit with gDNA Eraser (TaKaRa). The resulting complementary DNA (cDNA) yield was then subjected to PCR to examine the gene expression of alkaline phosphatase (ALP), type I collagen, osteocalcin (OC), Cbfa-1/Runx-2, and β-actin. Quantitative polymerase chain reaction (qPCR) was conducted using All-in-One qPCR Mix assay (Gene Copoeia). The gene expressions were quantified by calculating $2^{-\Delta CT}$ values, where $C_T$ represented the cycle number when an arbitrarily placed threshold was reached and $\Delta C_T = (C_{T,\text{ target gene}} - C_{T,\ \beta\text{-actin}})$.

***Calcium deposit detection***

A 2% (w/v) alizarin red solution was used to detect calcium deposits. The freeze-sectioned slice of cell-scaffold construct was covered with alizarin red solution for about 10 min and then rinsed with water and PBS solution.

***Statistical analysis***

All results were presented as means ± standard deviation (n=5). The unpaired form of the Student's t-test was applied to determine the significance level of differences. The results were analyzed by SPSS v 19.0 software, and a value of $p < 0.05$ was considered statistically significant.

## Results and Discussion

Figure 1 shows scanning electron microscopy (SEM) images of various scaffolds obtained via TIPS process. A three-dimensional pure PLLA nano-fibrous network was formed (Figure 1a and 1d) and the diameter of the fibers varied from 100 nm to 500 nm, within the same scale as natural collagen fibers. The sample of PLLA/CA was obtained by dissolving equal amounts of PLLA and CA in THF. As shown in Figure 1b and 1e, PLLA/CA exhibited different external and internal morphology. The surface morphology of PLLA/CA was similar to that of pure PLLA. However, the nanofiber inside the scaffold became shorter and uneven compared to PLLA sample, although the average diameter was similar. When 0.5% (w/v) CA solution was used for the solvent exchange process of PLLA/CA gel, the sample referred as PLLA/CA-CA exhibited similar nano-fibrous morphology on the surface as well as inside (Figure 1c and 1f). It has been known that the gelation stage during TIPS process was critical for the architecture of the scaffolds[32,33]. Different phase separation mechanisms and crystallization behavior account for the significant differences of PLLA morphology[4,9,10]. The introduction of CA may affect the phase separation and crystallization of PLLA, which is confirmed by the comparison of PLLA and PLLA/CA scaffolds . Furthermore, the current study suggested that the solvent exchange process from polymer-rich phase has also certain impact on the morphology of PLLA-based scaffolds.

Contact angle of water droplet was measured by sessile drop method on PLLA-based scaffolds for the evaluation of hydrophilic property. The measurement on the as-synthesized samples gave the contact angle for PLLA (128.2 ± 2.8°), PLLA/CA (90.7 ± 6.3°) and PLLA/CA-CA (74.4 ± 4.7°), respectively. Since the porous morphology may have certain effect on the contact angle measurement, all the samples were pressed into thin films to minimize the effects of porous surface morphology and the pressed samples were also tested. The average roughness of the pressed samples was confirmed by AFM measurement to be similar and less than 100 nm (PLLA: 79.19 ± 12.21 nm, PLLA/CA: 63.07 ± 18.79 nm, PLLA/CA-CA: 67.39 ± 8.45 nm). There was similar trend for the contact angle changes after CA treatment on either pressed or as-synthesized samples. As shown in Figure 2, the water contact angle of the pressed PLLA nano-fibrous scaffolds is much higher due to its hydrophobic nature. After modification with CA, the possible introduction of a strongly polar group (−COOH) on PLLA/CA surfaces decreased the contact angle and improved their hydrophilicity. In addition, using 0.5% CA solution for the solvent exchange process can further decrease the contact angle of PLLA/CA-CA sample. The PLLA/CA-CA samples were investigated in further studies due to their better hydrophilicity.

The crystalline structures of PLLA, PLLA/CA-CA and CA were further investigated by WAXD analysis (Figure 3). Based on the two strongest reflections from (110)/(200) and (203) in the WAXD pattern, corresponding to $2\theta = 16.4°$ and 18.8° respectively, the crystalline phase was characterized as the α′-form of PLLA[34]. From the pattern of the PLLA/CA-CA sample, no peaks of the polycondensation of L-lactic acid/citric acid oligomer (PLCA)[35] can be observed, ruling out the formation of covalent bonding between PLLA and CA. Most of the crystallization peaks in the WAXD pattern of PLLA/CA-CA (marked by *) were assigned to anhydrous citric acid (JCPDS Card No. 16-1157). In contrast, the crystallization of citric acid

hydrate (JCPDS Card No. 15-0985) occurred when pure CA solution was freeze-dried, as revealed by extra peaks (marked by ∆) in WAXD pattern of CA sample. As shown in Figure 3, the absence of triangle-labeled peaks and the increased or decreased intensity of asterisk-labeled peaks were confirmed to be caused by different CA crystallization process. The result suggested that certain interaction between PLLA and CA molecule led to the expelling of water from CA crystallization.

ATR-FTIR was used for the further characterization of PLLA-based nano-fibrous scaffolds due to its distinct absorption patterns in characteristic bands. Figure 4 shows ATR-FTIR spectra in the 3700-800 $cm^{-1}$ region of PLLA, PLLA/CA-CA and CA. The inset graph is the overlapped ATR-FTIR spectra in the 2000-800 $cm^{-1}$ region of PLLA and PLLA/CA-CA. The intensity of patterns of PLLA and PLLA/CA-CA were normalized according to the peak at 1453 $cm^{-1}$ due to C–H stretching in methyl groups[36]. From the spectrum of PLLA/CA-CA, the peaks at about 927 $cm^{-1}$, 1632 $cm^{-1}$ and a broad absorption band in the range of 3600-2500 $cm^{-1}$ came from CA molecule[37]. The absorption peak in the range of 3600-3400 $cm^{-1}$ was assigned to the stretching vibration band of O–H in carboxyl[35], which is considered as the most important factor for the improvement of the hydrophilicity of PLLA-based scaffolds. On the other hand, a broad absorption band around 2970 $cm^{-1}$ was assigned to the carbonyl in the state of hydrogen bond (···C=O) association with hydroxyl[38] which made the absorption band shift toward the lower wavenumber. The O–H and C=O bands between 3600-2500 $cm^{-1}$ in the PLLA/CA-CA sample were weaker compared to CA alone, which suggest that CA content in PLLA/CA-CA is relatively low.

In the IR spectrum of PLLA/CA-CA, the carbonyl stretching vibration [ν(C=O)] from PLLA at about 1757 $cm^{-1}$ showed a significant reduction in intensity and a new band appeared at about 1715 $cm^{-1}$ was assigned to C=O in the state of hydrogen bond association[39,40]. The new band is also different from C=O band at 1730 $cm^{-1}$ in the pattern of CA[41]. These results indicated that there were a certain number of hydrogen bond associations in PLLA/CA-CA. The hydrogen bond association between PLLA and CA may increase hydrophilicity, biocompatibility and mechanical properties of the scaffolds[42].

The stretching vibration of C–O–C bond and rocking vibration of $CH_3$ bonds are presented in the range of 1300-1000 $cm^{-1}$ [34]. As shown in the inset graph of Figure 4, the intensity of these absorption bands showed significant difference in PLLA/CA-CA compared to PLLA, which suggested some structural changes and chain reconstructions in PLLA/CA-CA[36]. Moreover, the stretching vibration mode of C–O–C [$\nu_{as}$(C–O–C)][43] at about 1189 $cm^{-1}$ became wider and a new relatively weak band appeared at 1247 $cm^{-1}$. This was considered as the shift of the combined peak at 1264 $cm^{-1}$ of C–O–C stretching vibration and C–H deformation vibration in PLLA[34] toward lower wavenumber due to the introduction of CA. This change of vibration from high to low energy mode suggested that the backbone vibration became more flexible in PLLA/CA-CA[44,45].

Figure 5 shows the typical SEM images of the morphology of mBMSCs adhesion on PLLA and PLLA/CA-CA scaffolds after 24 h culture. As shown in Figure 5a, the cell on PLLA scaffolds showed a spherical morphology with certain extent of cell spreading. In contrast, the cell showed extensive spreading on the PLLA/CA-CA scaffolds with many small processes interacting with substrate (Figure 5b). A quantitative measurement concerning the spreading area per cell was conducted based on SEM images. The difference in the cell spreading area of PLLA ($A_{PLLA}$=180.3 ± 36.8 $\mu m^2$ per cell, n=20) and PLLA/CA-CA ($A_{PLLA/CA-CA}$=378.9 ± 67.6 $\mu m^2$ per cell, n=20) is statistically significant (P<0.001). Combined with the results of contact angle measurement, this result demonstrated that PLLA/CA-CA scaffolds with a moderate hydrophilicity (contact angle of around 75°) were more beneficial for cell adhesion, compared to PLLA scaffolds (contact angle of around 130°). It is recognized that the adhesion and spreading of cells on a surface are strongly influenced by the extent of hydrophilicity/hydrophobicity. The cells had better spreading on surfaces with moderate hydrophilicity than those of either highly hydrophobic or highly hydrophilic[46]. Using the model of self-assembled monolayers (SAMs) of alkanethiols on gold, Hao et al.[47] observed that the spreading of human fetal MSCs (hMSCs) and mouse bone marrow MSCs (mBMSCs) were promoted on -OH/-$CH_3$ mixed hydrophilic SAMs with water contact angles of 20–70°. Our observation was generally in good consistency with these previous reports.

Cell viability was determined with a Live/Dead Viability/Cytotoxicity Assay Kit. The double color fluorescent staining assay was performed following the manufacturer's instruction on days 1, 4 and 7. As shown in Figure 6, most of the cells on both PLLA and PLLA/CA-CA scaffolds showed an excellent cell activity (Figure 6a: 95.7%, 6b: 89.8%, 6c: 97.3%, 6d: 99.1%, 6e: 98.4% and 6f: 99.9%). This further confirmed PLLA-based scaffolds have good biocompatibility and have little or no toxicity to mBMSCs. It was noted that there were more cells on PLLA scaffolds than that on PLLA/CA-CA scaffolds on day 1 (Figure 6a and 6b). Nonetheless, after culturing for 4 days (Figure 6c and 6d) and 7 days (Figure 6e and 6f), a greater amount of cells can be observed on PLLA/CA-CA scaffolds.

Cell proliferation was quantitatively examined using Cell Counting Kit-8 (CCK-8) assay on PLLA and PLLA/CA-CA scaffolds after cultured for 2, 5 and 8 days. As shown in Figure 7, a significant increase in cell number was observed on both PLLA and PLLA/CA-CA scaffolds, which indicated that PLLA-based scaffolds have good biocompatibility and were suitable for cell attachment and proliferation. On day 2, mBMSCs on PLLA scaffolds showed a greater amount than that on PLLA/CA-CA scaffolds, consistent with the fluorescent observation on the differences in initial adherent cell number on day 1. After culturing for 5 days and 8 days, a faster proliferation rate and a greater amount of cells can be observed clearly on PLLA/CA-CA scaffolds than that on PLLA scaffolds. This may be because that in the initial stage of cell culture, the local concentrations of –COOH on the surface of PLLA/CA-CA scaffolds was too high. The excessive acidity on the surface could be detrimental to cell growth. With the increasing of culture time, however, PLLA/CA-CA provided a more suitable surface for cell proliferation.

As a standard osteogenic differentiation marker, alkaline

phosphatase (ALP) was detected with BCIP/NBT staining on the cell-scaffold constructs after cultured with osteogenic supplements for 7 and 14 days. The constructs cultured without osteogenic supplements were also tested as controls. As shown in Figure 8a and Figure 8d, the negative staining of ALP activity on control samples suggested that the materials themselves had no ability to promote osteogenic differentiation of mBMSCs. Under osteogenic induction conditions, however, all of the cell-scaffold constructs (Figure 8b-c and Figure 8e-f) showed a positive staining (in the blue-violet region), which indicated that both PLLA and PLLA/CA-CA scaffolds were suitable for the osteogenic differentiation of mBMSCs in osteogenic supplements. In general, the staining in PLLA/CA-CA scaffolds was qualitatively more intense than that in PLLA scaffolds although a quantitative analysis was unavailable.

To quantitatively evaluate the ALP activity of the cells, pNPP assay was performed after the cell-scaffold constructs being cultured with osteogenic supplements for 7 and 14 days. As shown in Figure 9, an increasing trend of ALP activity of the cells can be observed from 7d to 14d, especially on PLLA/CA-CA scaffolds. There was a slight but not statistically significant increase on PLLA scaffolds. Furthermore, the cells on PLLA/CA-CA scaffolds displayed significantly higher levels (nearly doubled on day 14) of ALP activity, suggesting that the modified scaffold had enhanced promotion on the osteogenic differentiation of mBMSCs.

Gene expression of bone-relevant markers such as alkaline phosphatase (ALP), type I collagen (COL), osteocalcin (OCN) and Runx-2/Cbfa-1 in mBMSCs were determined by real-time RT-PCR at Day 21 and Day 28. β-actin was used as the house-keeping gene, and the validated primer sequences are shown in Table 1.

Table 1: Validated primer sequences for real-time PCR

| Gene | | Primer sequences (5'-3') |
|---|---|---|
| ALP | sense | TGCCTACTTGTGTGGCGTGAA |
| | antisense | TCACCCGAGTGGTAGTCACAATG |
| COL | sense | ATGCCGCGACCTCAAGATG |
| | antisense | TGAGGCACAGACGGCTGAGTA |
| OCN | sense | AGCAGCTTGGCCCAGACCTA |
| | antisense | TAGCGCCGGAGTCTGTTCACTAC |
| Runx2/ Cbfa-1 | sense | CACTGGCGGTGCAACAAGA |
| | antisense | TTTCATAACAGCGGAGGCATTTC |
| β-actin | sense | TGACAGGATGCAGAAGGAGA |
| | antisense | GCTGGAAGGTGGACAGTGAG |

As shown in Figure 10, cells cultured on PLLA scaffolds showed relatively stable expression of ALP and COL from 21d to 28d. In contrast, the expressions of the ALP and COL genes were lower on PLLA/CA-CA scaffolds and had a decreasing trend from 21d to 28d. Since ALP is generally considered as a marker for the early stage osteogenic differentiation of mBMSC, taking together the ALP staining and activity evaluation on 7d and 14d cultures, the hydrophilic PLLA/CA-CA scaffolds appeared to promote the osteogenic differentiation of mBMSC earlier than the pure PLLA scaffolds. COL holds overwhelming majority among the bony structural proteins and provides templates for mineralization, which is also considered as a marker for the early stage osteogenic differentiation of mBMSC[48]. The expression of COL showing the same trend with ALP, which further indicated that PLLA/CA-CA promote the osteogenic differentiation of mBMSC earlier than PLLA. This promotion effect was further confirmed by the expression of OCN gene which is a typical marker for the late stage of osteogenic differentiation of mBMSC. The cells cultured on PLLA/CA-CA scaffolds had significantly higher expression of OCN and Runx-2 genes on 28d than that on PLLA and the expression exhibited significant increase from 21d to 28d.

After being cultured with osteogenic supplements for 10 and 18 days, as another marker of osteogenic differentiation, calcium deposition by cells was assessed with alizarin staining. As shown in Figure 11a and 11d, the control samples without osteogenic induction showed no calcium deposition. However, after 10 and 18 days of culture with osteogenic supplements, significant calcium staining (red-orange regions) were observed from cells cultured on the both scaffolds (Figure 11b-c and Figure 11 e-f). The results showed promise of these PLLA-based scaffolds for bone tissue engineering.

## Conclusions

Citric acid (CA) was introduced into PLLA nano-fibrous scaffolds preparation during TIPS process. The hydrogen bond association occurred between PLLA and CA molecules. The modification with a strongly polar group (–COOH) on PLLA surface decreased the contact angle and improved its hydrophilicity to a more suitable range for cell culture. The modified scaffolds enhanced cell affinity and were beneficial for cell adhesion and spreading. The cell proliferation rate and cell activity had increased significantly on CA modified PLLA scaffolds. The hydrophilic modification of PLLA scaffolds promoted osteogenic differentiation of mBMSCs and was thus promising for bone regeneration applications.

## Acknowledgements

The work is supported in part by the National Basic Research Program of China (2012CB619100), National Natural Science Foundation of China (51072056), Program for Changjiang Scholars and Innovative Research Team in University (IRT 0919), Key Grant of Chinese Ministry of Education (313022) and the 111 Project (B13039).

## Notes and references

[a] *School of Materials Science and Engineering, South China University of Technology, Guangzhou 510641, PR China.*
[b] *National Engineering Research Center for Tissue Restoration and Reconstruction, Guangzhou 510006, P.R. China*
*E-mail: duchang@scut.edu.cn; Tel: 86-020-22236062*

[c] *SZU-NUS Collaborative Innovation Center for Optoelectronic Science and Technology, and Key Laboratory of Optoelectronic Devices and Systems of Ministry of Education and Guangdong Province, College of Optoelectronic Engineering, Shenzhen University, Shenzhen 518060, P.R. China.*

1 M. M. Stevens, J. H. George. *Science*, 2005, 310, 1135-1138.
2 S. Zhang. *Nature biotechnology*, 2003, 21, 1171-1178.
3 K. M. Woo, J. Jun, V. J. Chen, *et al*. *Biomaterials*, 2007, 28, 335-343.
4 J. Shao, C. Chen, Y. Wang, *et al*. *Polymer Degradation and Stability*, 2012, 97, 955-963.
5 L. A. Smith, P. X. Ma. *Colloids and surfaces B: biointerfaces*, 2004, 39, 125-131.
6 A. Nur-E-Kamal, I. Ahmed, J. Kamal, *et al*. *Biochemical and biophysical research communications*, 2005, 331, 428-434.
7 F. A. Sheikh, M. A. Kanjwal, H. Y. Kim, *et al*. *Applied Surface Science*, 2010, 257, 296-301.
8 P. X. Ma. *Advanced drug delivery reviews*, 2008, 60, 184-198.
9 J. Shao, C. Chen, Y. Wang, *et al*. *Applied Surface Science*, 2012, 258, 6665-6671.
10 J. Shao, C. Chen, Y. Wang, *et al*. *Reactive and Functional Polymers*, 2012, 72, 765-772.
11 Z. Zhang, J. Hu, P. X. Ma. *Advanced drug delivery reviews*, 2012, 64, 1129-1141
12 E. D. Hay. Cell biology of extracellular matrix. 2nd edition, New York: Plenum Press; 1991.
13 D. K. Han, J. A. Hubbell. *Macromolecules*, 1997, 30, 6077-6083.
14 A. D. Cook, U. B. Pajvani, J. S. Hrkach, *et al*. *Biomaterials*, 1997, 18, 1417-1424.
15 T. Groth, G. Altankov, K. Kolsz. *Biomaterials*, 1994, 15, 423-428.
16 M. J. Dalby, S. Childs, M. O. Riehle, *et al*. *Biomaterials*, 2003, 24, 927-935.
17 I. D. Xynos, M. V. J. Hukkanen, J. J. Batten, *et al*. *Calcified Tissue International*, 2000, 67, 321-329.
18 C. Loty, J. M. Sautier, M. T. Tan, *et al*. *Journal of Bone and Mineral Research*, 2001, 16, 231-239.
19 I. D. Xynos, A. J. Edgar, L. D. K. Buttery, *et al*. *Biochemical and biophysical research communications*, 2000, 276, 461-465.
20 D. I. Hay, E. C. *Moreno. Journal of dental research*, 1979, 58, 930-942.
21 S. N. Stephansson, B. A. Byers, A. J. Garcia. *Biomaterials*, 2002, 23, 2527-2534.
22 A. G. Mikos, M. D. Lyman, L. E. Freed, *et al*. *Biomaterials*, 1994, 15, 55-58.
23 J. P. Chen, C. H. Su. *Acta biomaterialia*, 2011, 7, 234-243.
24 Y. L. Cui, A. D. Qi, W. G. Liu, *et al*. *Biomaterials*, 2003, 24, 3859-3868.
25 K. Madhavan Nampoothiri, N. R. Nair, R. P. John. *Bioresource technology*, 2010, 101, 8493-8501.
26 J. P. Chen, C. H. Su. *Acta biomaterialia*, 2011, 7, 234-243.
27 Y. Zhu, C. Gao, X. Liu, *et al*. *Tissue engineering*, 2004, 10, 53-61.
28 R. Morent, N. De Geyter, C. Leys, *et al*. *Surface and Coatings Technology*, 2007, 201, 7847-7854.
29 L. Lei, T. Ding, R. Shi, *et al*. *Polymer Degradation and Stability*, 2007, 92, 389-396.
30 J. Yang, A. R. Webb, S. J. Pickerill, *et al*. *Biomaterials*, 2006, 27, 1889-1898.
31 P. X. Ma, R. Zhang. *Journal of biomedical materials research*, 1999, 46, 60-72.
32 G. Wei, P. X. Ma. *Journal of Biomedical Materials Research Part A*, 2006, 78, 306-315.
33 M. J. Gupte, P. X. Ma. *Journal of Dental Research*, 2012, 91, 227-234.
34 P. Pan, B. Zhu, W. Kai, *et al*. *Macromolecules*, 2008, 41, 4296-4304.
35 F. Yao, Y. Bai, W. Chen, *et al*. *European polymer journal*, 2004, 40, 1895-1901.
36 N. T. Paragkumar, D. Edith, J. L. Six. *Applied Surface Science*, 2006, 253, 2758-2764.
37 H. Groen, K. J. Roberts. *The Journal of Physical Chemistry B*, 2001, 105, 10723-10730.
38 Z. Gu, R. Zambrano, A. McDermott. *Journal of the American Chemical Society*, 1994, 116, 6368-6372.
39 L. Zhang, X. Deng, S. Zhao, *et al*. *Polymer*, 1997, 38, 6001-6007.
40 L. Zhang, S. H. Goh, S. Y. Lee. *Polymer*, 1998, 39, 4841-4847.
41 R. Shi, Z. Zhang, Q. Liu, *et al*. *Carbohydrate Polymers*, 2007, 69, 748-755.
42 J. Yang, A. R. Webb, G. A. Ameer. *Advanced Materials*, 2004, 16, 511-516.
43 G. Kister, G. Cassanas, M. Vert. *Polymer*, 1998, 39, 267-273.
44 N. T. Paragkumar, D. Edith, J. L. Six. *Applied Surface Science*, 2006, 253, 2758-2764.
45 T. Furukawa, H. Sato, R. Murakami, *et al*. *Polymer*, 2007, 48, 1749-1755.
46 J. H. Lee, S. J. Lee, G. Khang, *et al*. *Journal of colloid and interface science*, 2000, 230, 84-90.
47 L. J. Hao, H. Yang, C. Du, *et al*. *Journal of Materials Chemistry B*, 2014, 2, 4794-4801.
48 X. Shi, Y. Wang, R. R. Varshney, *et al*. *European Journal of Pharmaceutical Sciences*, 2010, 39, 59-67.

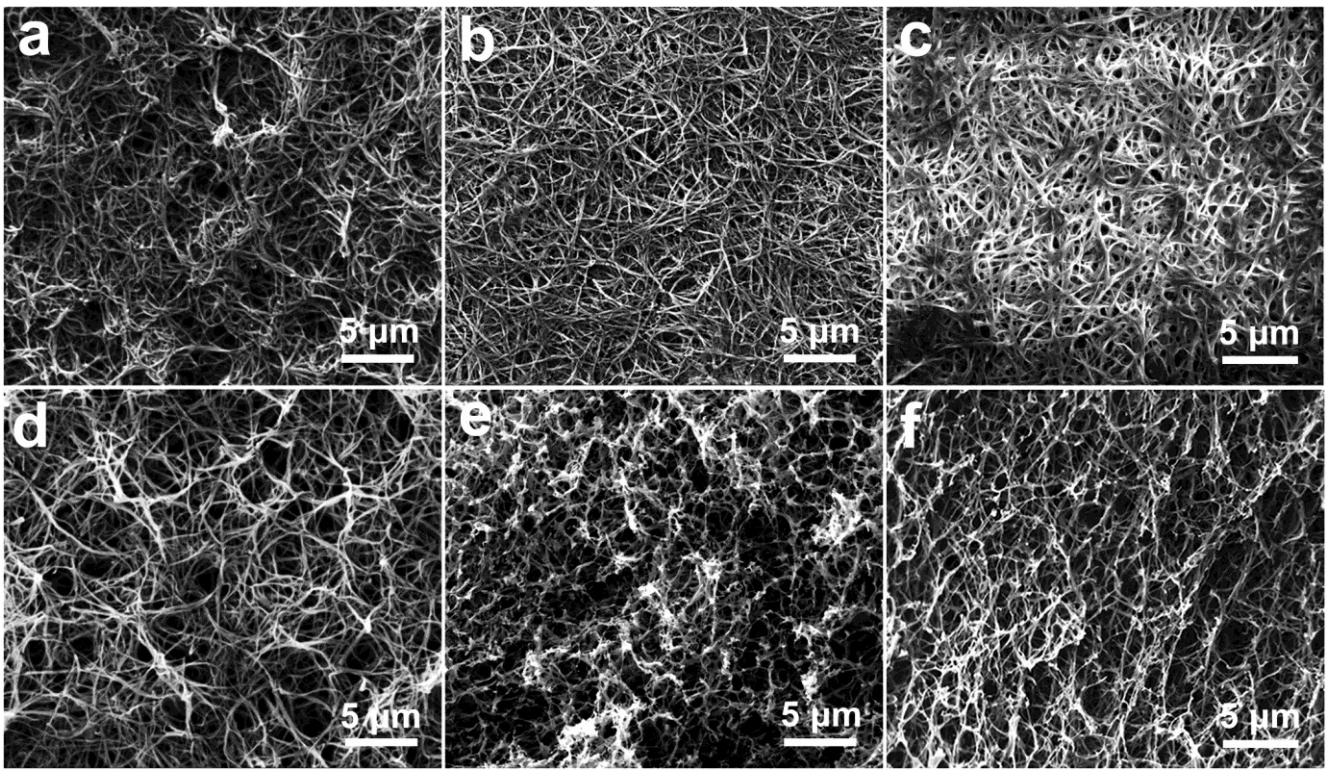


Figure 1: Typical SEM images of the external morphology (a, b, c) and the corresponding internal morphology (d, e, f) of PLLA-based nano-fibrous scaffolds: (a, d) PLLA, (b, e) PLLA/CA and (c, f) PLLA/CA-CA.

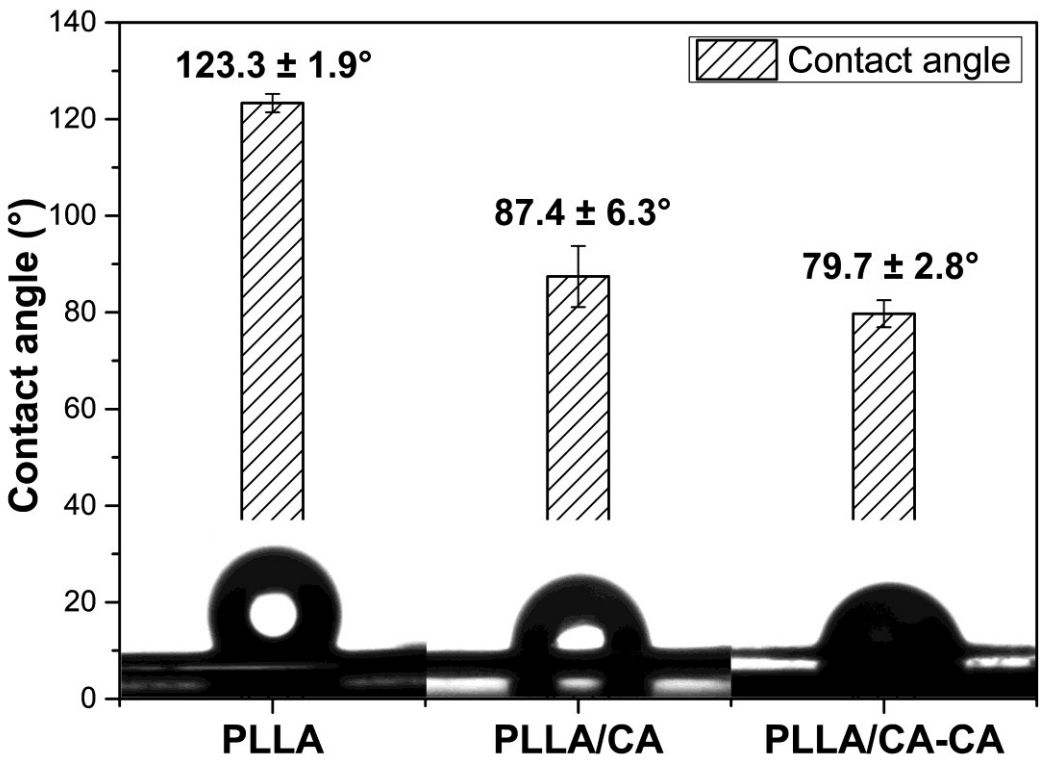


Figure 2: Contact angle measurement of PLLA, PLLA/CA and PLLA/CA-CA samples.

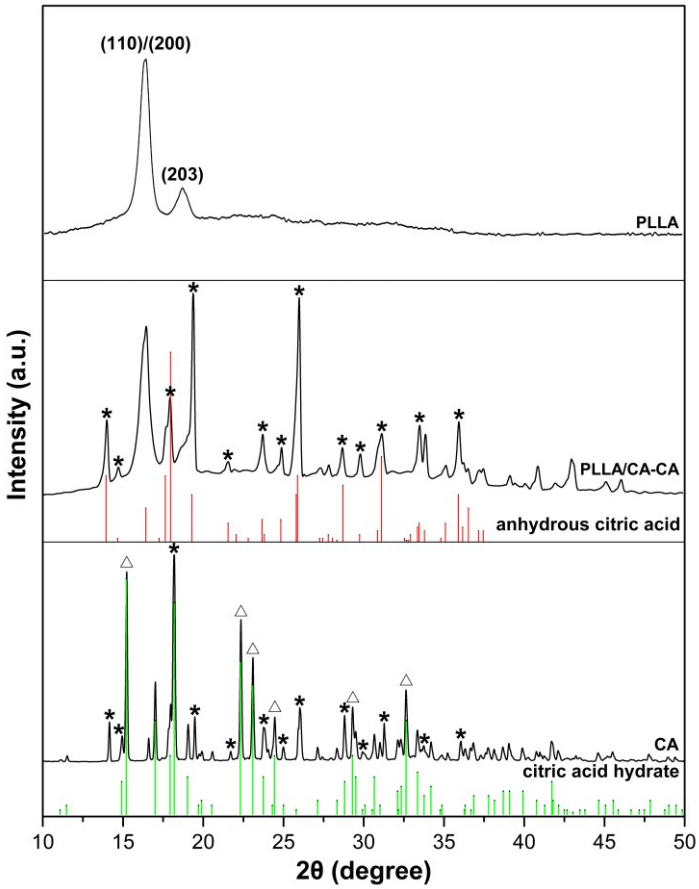


Figure 3: WAXD patterns of the PLLA, PLLA/CA-CA and CA samples. The vertical red lines and green lines at the bottom represent XRD peaks of pure anhydrous citric acid (JCPDS Card No. 16-1157) and citric acid hydrate (JCPDS Card No. 15-0985) respectively.

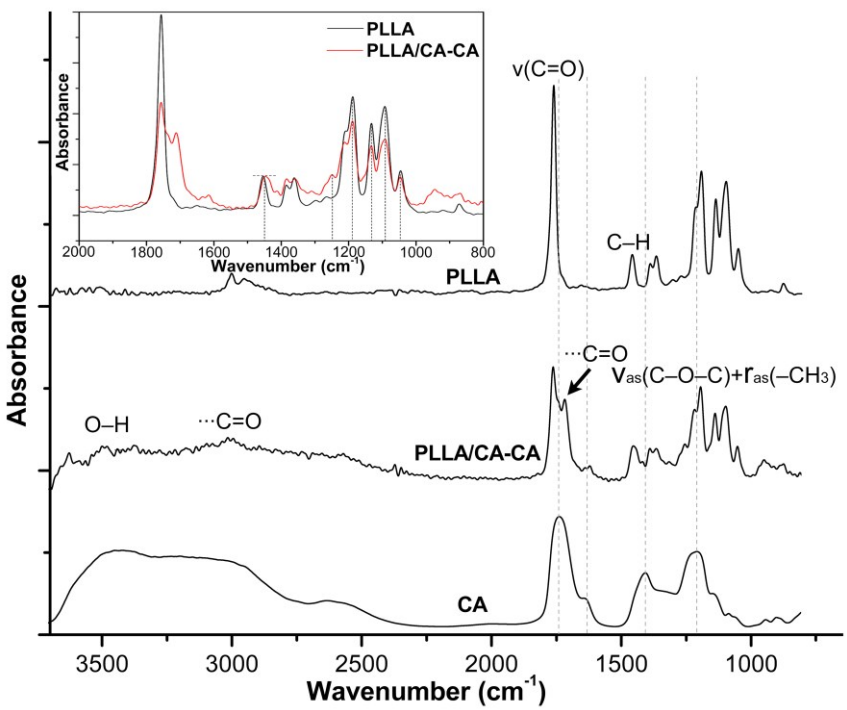


Figure 4: ATR-FTIR spectra of the PLLA, PLLA/CA-CA and CA samples. The inset graph is the overlapped ATR-FTIR spectra in the 2000-800 $cm^{-1}$ region of PLLA and PLLA/CA-CA.

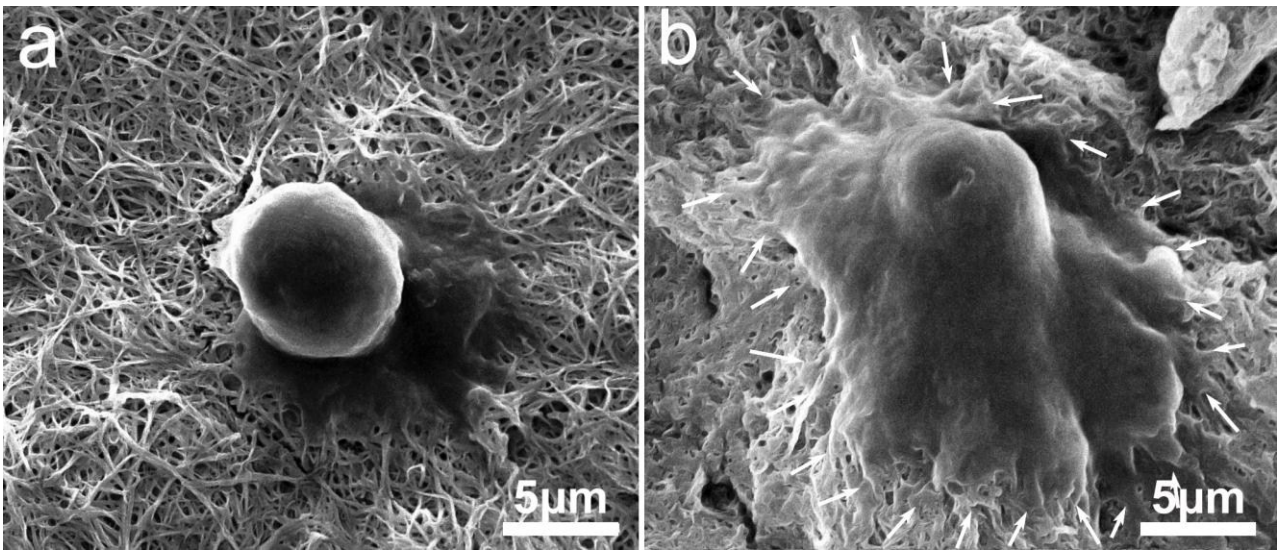


Figure 5: Typical SEM morphology of the cells attached on the (a) PLLA and (b) PLLA/CA-CA scaffolds. White arrows in (b) indicate the cellular processes interacting with substrate.

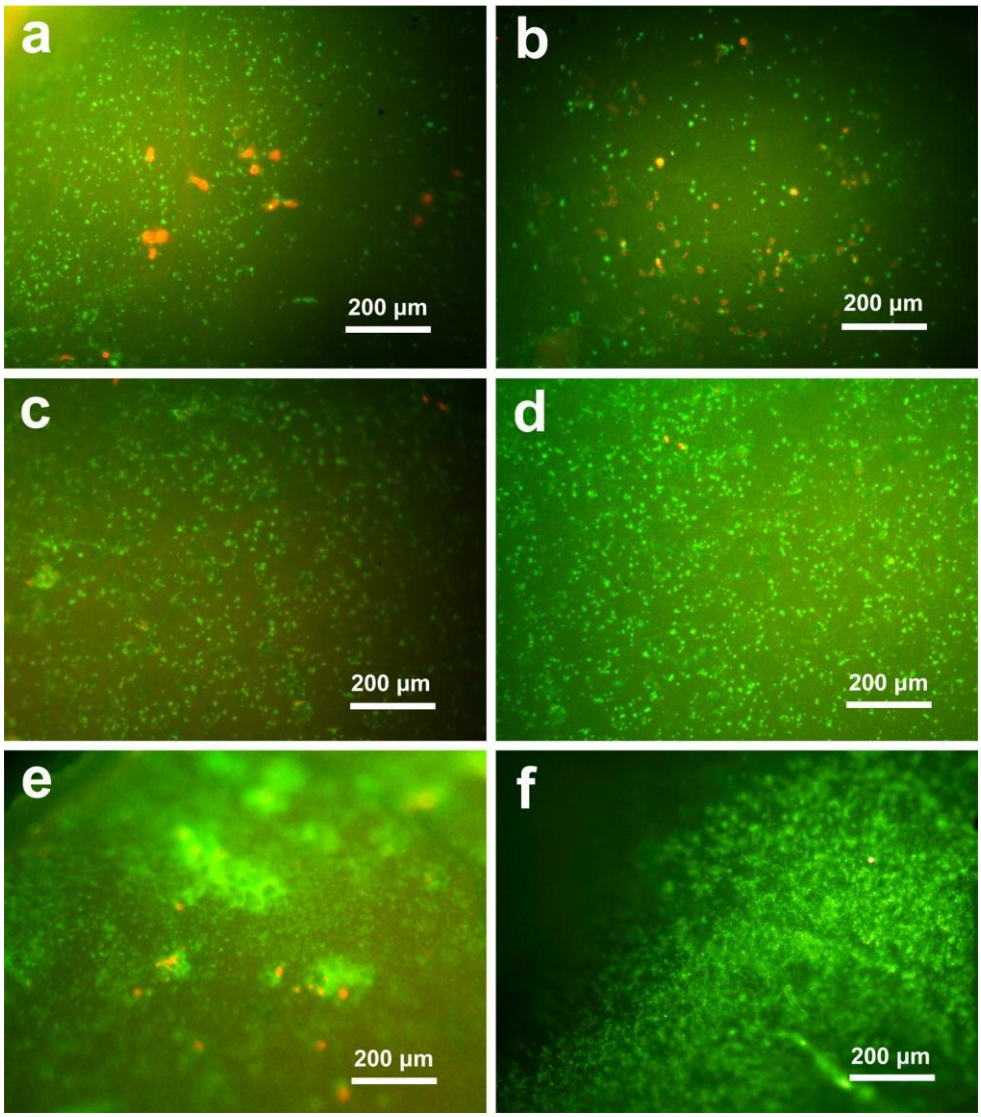


Figure 6: Live/Dead assay of mBMSCs growth on (a, c, e) PLLA and (b, d, f) PLLA/CA-CA scaffolds for (a, b) 1 day, (c, d) 4 days, and (e, f) 7 days. Green color indicated the active cells and red color showed the dead.

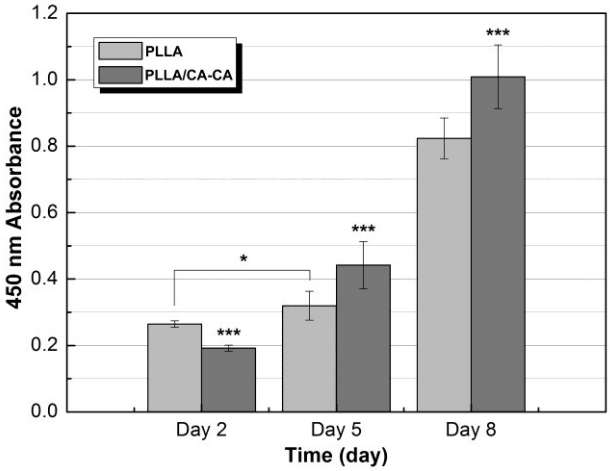


Figure 7: mBMSC proliferation on PLLA and PLLA/CA-CA scaffolds ($^{*}p<0.05$ for the Day 5 sample compared to the Day 2 sample, $^{***}p<0.001$ for the PLLA/CA-CA samples compared to the corresponding PLLA samples).

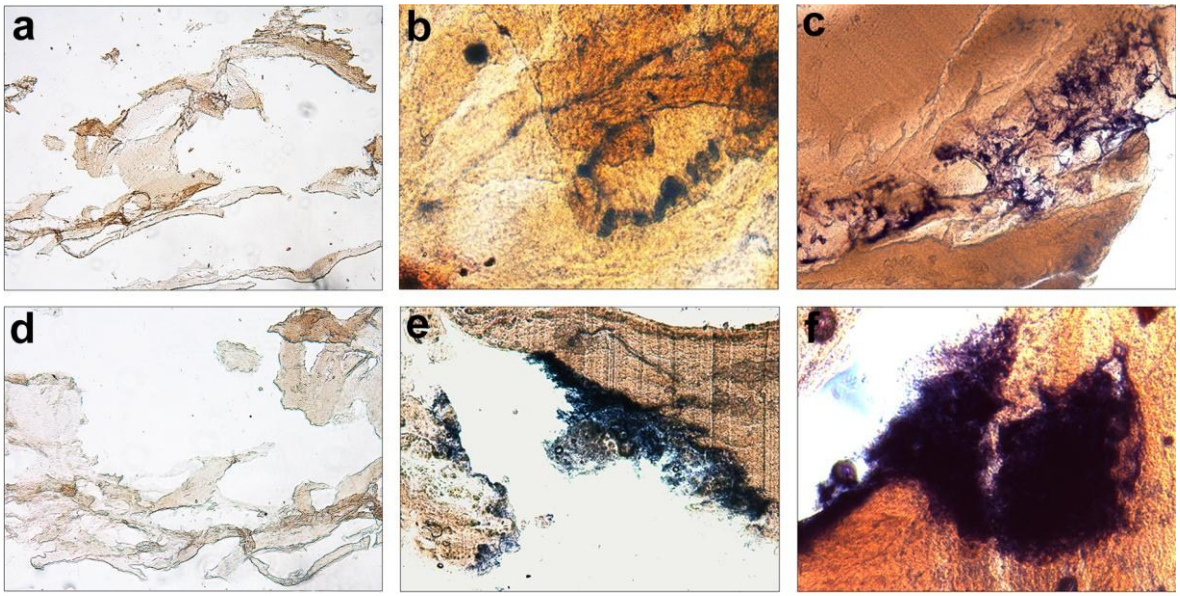


Figure 8: ALP staining of cells on (a, d) control group, (b, e) PLLA and (c, f) PLLA/CA-CA scaffolds for 7 days (a, b, c) and 14 days (d, e, f). The cells cultured without osteogenic supplements on PLLA/CA-CA scaffolds were used as controls.

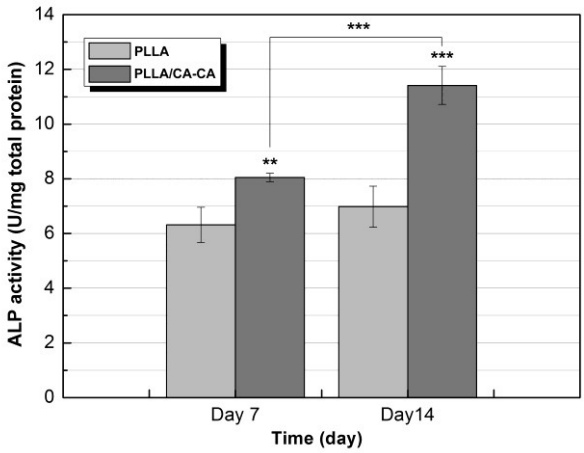


Figure 9: Alkaline phosphatase activity of cells cultured on PLLA and PLLA/CA-CA scaffolds with osteogenic supplements (The asterisks above PLLA/CA-CA samples indicated differences compared to the PLLA samples at the same time point. $^{**}p<0.01$, $^{***}p<0.001$).

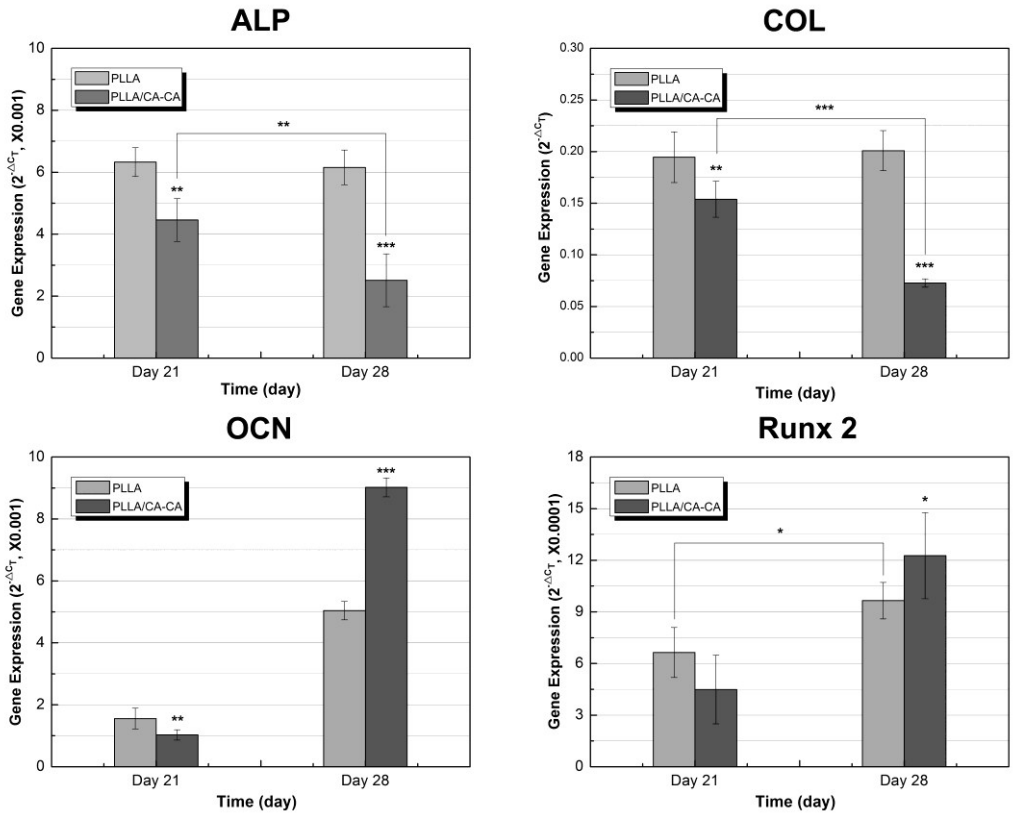


Figure 10: Osteogenic gene expression of cells on PLLA and PLLA/CA-CA scaffolds for 21 and 28 days (The asterisks above PLLA/CA-CA samples indicated differences compared to the PLLA samples at the same time point. $^{*}p<0.05$, $^{**}p<0.01$, $^{***}p<0.001$).

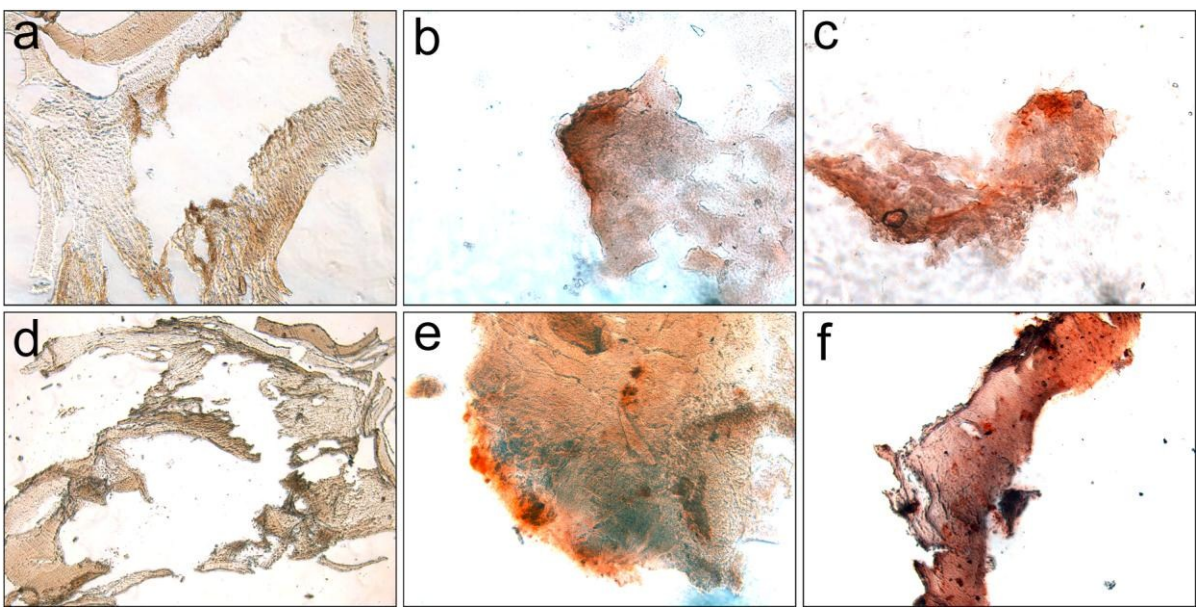


Figure 11: Alizarin staining of calcium deposition by mBMSC on (a, d) control group, (b, e) PLLA and (c, f) PLLA/CA-CA scaffolds for 10 days (a, b, c) and 18 days (d, e, f). The control samples without osteogenic induction showed negative results.

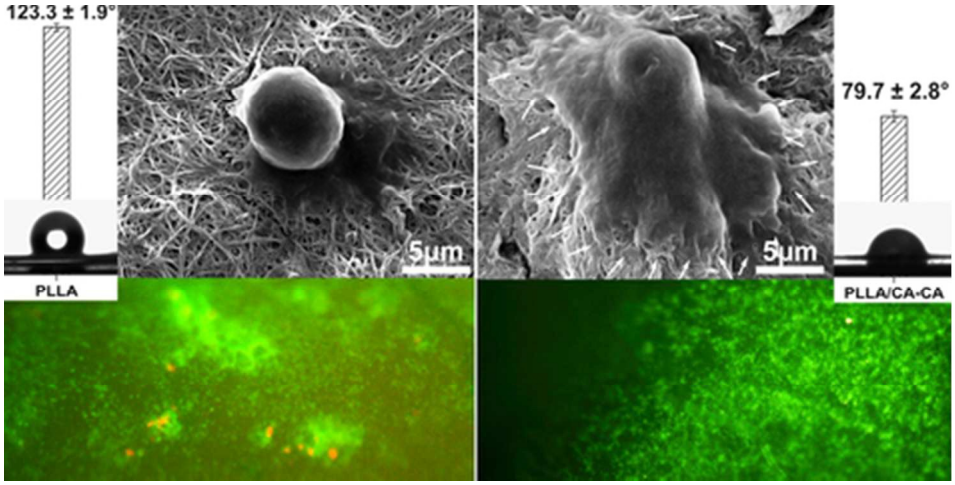


40x20mm (300 x 300 DPI)